

## RATE DEPENDENT FRACTURE BEHAVIOUR OF ADHESIVELY BONDED JOINTS

I. GEORGIOU, A. IVANKOVIC, A. J. KINLOCH AND V. TROPSA

*Imperial College London, Department of Mechanical Engineering,  
South Kensington campus, London, SW7 2AZX, UK*

### ABSTRACT

Standard small-scale peel tests, such as the impact wedge-peel (IWP–ISO 11343) and T-peel tests are often employed to analyse the fracture behaviour of structural adhesives. The current work aims to examine the behaviour of adhesively bonded joints under various loading rates by conducting a series of peel tests and simulating the results from such tests numerically. In all tests, thin sheets of aluminium alloy substrates were bonded together using ‘XD4600’ and ‘XD1493’ structural epoxy-adhesives. Numerical modelling of the tests was conducted using the Finite Volume (FV) method. For this purpose, transient, 3D, procedures were developed including a newly developed contact model and a cohesive zone (CZ) model as a local failure criterion. The CZ model was defined using two materials parameters, the adhesive fracture energy,  $G_c$ , and the maximum cohesive stress,  $\sigma_m$ . In order to measure the adhesive fracture energy tapered double cantilever beam (TDCB) tests were performed, whereas the value of  $\sigma_m$  was estimated from the stress-strain curves at corresponding rates and taken to be the ultimate tensile strength (UTS). Numerical analysis of the tests was conducted in order to calibrate the traction separation curves at various rates, and to examine the stick-slip crack behaviour which appeared in TDCB specimens with ‘XD4600’ adhesive tested at high rates. The calibrated CZ curves were then used in the prediction of failures in the IWP specimens. Work on modelling T-peel tests is currently in progress.

### KEYWORDS

Adhesive, cohesive zone model, finite volume method, impact wedge peel test, TDCB.

### INTRODUCTION

Due to the environmental impact of motor vehicles, automotive manufacturing companies are being encouraged to produce lighter and more fuel-efficient vehicles. Vehicle structure offers an appropriate scope for potential weight saving, with the body-in-white (BIW)

providing the largest contribution through the use of new technologies or new lightweight materials. Note that BIW is a conventional name adopted by automotive engineers to represent the body/chassis structure along with any exterior skin panels such as bonnet, boot lids, etc. Recent developments have revealed that up to 30% reduction of the total weight of the car can be achieved by substituting steel with aluminium alloy [1]. However, the substitution of one material by another may give rise to various problems, and one of them is the method of joining. The current research will investigate the application of adhesive bonding as a possible solution to the above challenge.

An important feature of any vehicle structure is its behaviour under impact loading. Adhesives for automotive applications are based on structural toughened-epoxy polymers that exhibit viscoplastic deformations, and therefore a strain-rate sensitivity. Under impact loading, adhesive joints may fail in a brittle manner. As a consequence, the surrounding body panel material would be unable to undergo substantial plastic deformation, which would result in a low dissipated energy at impact. Hence, the reliability of the adhesively bonded joints, when they are used in safety-critical areas, is of primary importance to the automotive industry. The present work aims to investigate the mechanical and fracture behaviour of adhesively bonded joints under various loading rates.

## EXPERIMENTAL PROCEDURES

### *Materials tested*

*Substrates.* Two commercial aluminium alloys (see Table 1), received as hot-rolled sheets (from ALCAN), were the main body-panel materials used in the current work. The thickness of the sheets varied from 1 to 3 mm for the 5754-O alloy and from 1 to 2 mm for the 6111-T6 alloy. For the tapered double-cantilever beam (TDCB) tests, where the substrates should remain within the elastic region, a high yield strength alloy, 2014, was used throughout. The specimens were prepared and pre-treated prior to bonding using the procedures proposed by Blackman *et. al.* [2]. The chemical compositions of the alloys employed are given in Table 1.

Table 1. Chemical composition (wt%) of substrates used in the present work

Alloy	Si	Fe	Cu	Mn	Mg	Cr	Zn	Ti
5754-O	0.4	0.4	0.1	0.5	2.6-3.6	0.3	0.2	0.15
6111-T4	0.7-1.1	0.4	0.5-0.9	0.15-0.45	0.5-1.0	0.1	0.15	0.10
2014	0.5-0.9	0.5	3.9-5.0	0.40-1.20	0.2-0.8	0.1	0.25	0.15

Notes:

- (1) Balance is aluminium.
- (2) 2014 also contains 0.1% Nickel

*Adhesives.* Two single part, rubber toughened hot cured structural epoxy adhesives were used throughout the current research. Both adhesives were provided by Dow Automotive, Europe. The glass transition temperature,  $T_g$ , as well as the curing cycle employed for each adhesive are given in Table 2.

### *Mechanical Testing*

Uniaxial tensile tests were conducted to obtain the basic mechanical properties of the substrate materials and adhesives for a wide range of test rates. For testing of the substrate materials dog-bone specimens of 30 mm gauge length were machined from the sheets according to the ASTM (E8m-89b) standard [3]. Prior to testing, aluminium specimens were heat treated for 30 minutes at 180°C, simulating the adhesive curing process. A

standard dumb-bell shaped specimen of 30 mm gauge length was employed for the testing of the adhesives according to ASTM D 638-72 [4]. Specimens were machined following the EN ISO 2818:1996 standard [5] from a bulk 4 mm thick plate, and prepared according to the BS ISO 15166-1:1998 standard [6].

**Table 2.** Adhesives used in the current research

Adhesive	Form	Cure Temperature [°C]	Cure time [min]	T <sub>g</sub> [°C]
'XD4600'	Single-part	150-190*	15	113
'XD1493'	Single-part	180	30	91

(\*) 'XD4600' adhesive requires a heat curing at two different temperatures indicated above for the time of 15 min. at each.

#### *Tapered Double Cantilever Beam (TDCB) Tests*

The TDCB test configuration was employed to determine the adhesive fracture energy, G<sub>c</sub>. Tests were conducted at different crosshead speeds between 10<sup>-6</sup> and 1 m/s. A schematic of the test specimen is illustrated in Fig. 1(a). Due to symmetry only half of the specimen is considered in the numerical analysis, Fig. 1(b). The profile of the arms is machined such that the rate of compliance increases linearly with the crack length and hence the derivative of the compliance with crack length remains constant. The beams are contoured to the profile described by Eqn. 1 [2], where h is the height of the beam, a is the crack length and m is a constant ( $m = 2000 \text{ m}^{-1}$  in the present work).

$$m = \left\{ \frac{3a^2}{h^3} + \frac{1}{h} \right\} \quad (1)$$

The thickness of the TDCB specimens ( $B = 10 \text{ mm}$ ) is sufficient to ensure plain strain conditions. It should be noted that during the test the arms remain within their elastic limit. Therefore, from simple beam theory [7], and by the use of linear elastic fracture mechanics, the strain energy release rate of the adhesive can be obtained using Eqn. 2, where P is the load at failure and E<sub>s</sub> is the substrate modulus. The calculated adhesive fracture energy was employed in the simulation of the TDCB and impact wedge-peel (IWP) tests.

$$G_c = \frac{4P^2m}{E_s B^2} \quad (2)$$

#### *Impact Wedge Peel (IWP) Tests*

To study the fracture behaviour of the selected structural adhesive joints, impact wedge-peel tests (ISO 11343 [9]) were also conducted using a high-performance servo-hydraulic Instron machine. The test speed was varied between 0.4 and 11 m/s to investigate the effect of the rate on the cleavage force. A schematic representation of the impact wedge peel (IWP) test specimen is shown in Fig. 1(c), with its numerical representation given in Fig. 1(d). A wedge is pulled through the adhesive joint, which is shaped like a tuning fork. The substrates, cut out from aluminium sheets (1, 2 and 3 mm thick), were prepared prior to bonding and bonded together over a length of 30 mm. The excess of adhesive that was present at the 'V' formed by substrates was carefully removed before curing to keep a minimum bead of adhesive in this region. High-speed photography was also employed with a number of tests to show clearly the characteristic events during impact, i.e. wedge/specimen contact, crack initiation and propagation, bouncing of the arms, etc. A Kodak HS 4540 camera [10] fitted with a 135 mm Nikon lens was focused on the stationary wedge at a slight angle, in order to have a clear view of the crack propagation.

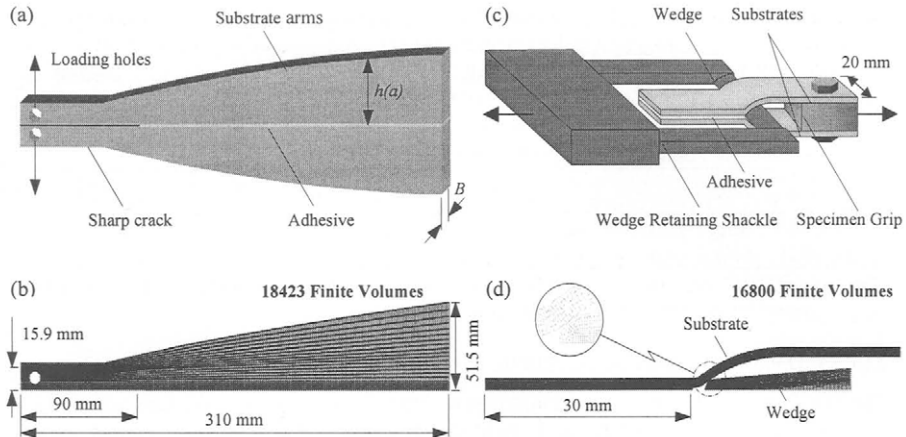


Fig. 1: Schematic of the: (a) TDCB test specimen; (b) FV representation of the TDCB geometry; (c) IWP test specimen; (d) FV representation of the IWP geometry. A bond line thickness of 0.4 mm is used for all test specimens.

#### *T-peel Tests*

A series of T-peel tests was conducted at 1, 5 and 50 mm/min in order to investigate the effect of the test rate on the average peeling force. A schematic of the test geometry is illustrated in Fig. 2. Symmetrical 90° peel test specimens were fabricated using rectangular substrate ( $20 \pm 0.25$  mm  $\times$   $300 \pm 1$  mm) cut from aluminium sheets of different thickness and bonded by structural adhesives. From the measured peel forces, and by employing an analytical elastic-plastic approach, the value of adhesive fracture energy  $G_c$  was measured [8].

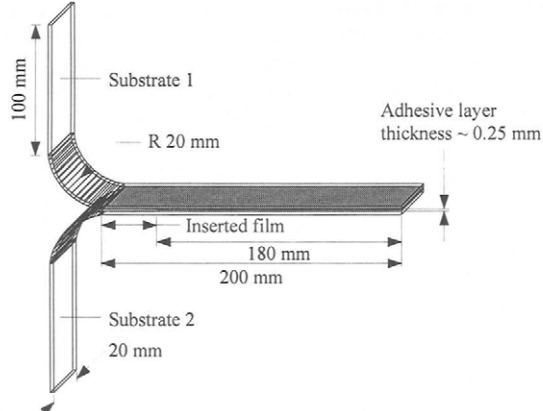


Fig. 2: Schematic of the T-peel test geometry.

#### FINITE VOLUME METHODOLOGY

A finite volume (FV) approach was used for the numerical simulation of the experiments [11]. The model was implemented using the ‘FOAM’ package, i.e. a C++ library for

continuum mechanics [12]. Schematics of the FV representation of the TDCB and IWP test specimens can be seen in Fig. 1(b) and (d) respectively. In the numerical analysis, the equation governing linear momentum is solved while Hooke's law was used to describe the behaviour of both bulk adhesive and substrate materials. This approach is only suitable for modelling linear elastic TDCB tests, and the finite strain plasticity is required for modelling of the T-peel and the IWP tests. Indeed, our current work is concerned with the peel tests. The CZ model was employed to describe the traction-separation behaviour of the adhesive material along the prospective crack path. The CZ model represents a local failure mechanism of the material. In the present work, only mode I failure was considered due to symmetry conditions, and the normal separation distance was related to the normal tractions via a Dugdale-like curve (Fig. 3). Particular care was taken to achieve mesh independent results.

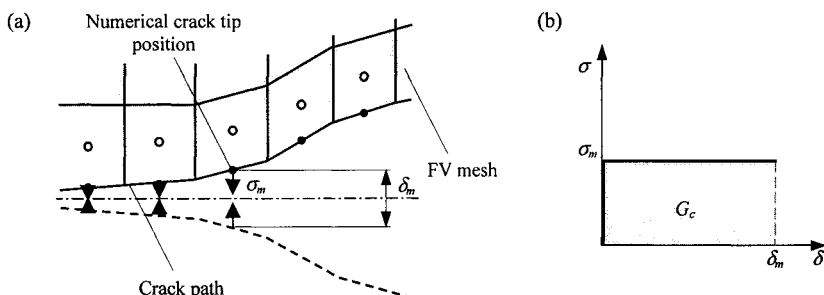


Fig. 3: (a) Schematic of the FV CZ model; (b) Dugdale traction-separation curve used in the analysis.

Early in the process the cohesive surfaces behave as the surrounding bulk material. After the stress level reaches its maximum value,  $\sigma_m$ , the material is irreversibly damaged. Since no direct measure of  $\sigma_m$  was available, this value was assumed to be equal to the ultimate tensile strength (UTS) of the adhesive. However, as it will be shown in Section 'Calibration of CZ model parameter  $\sigma_m$ ', the results are not very sensitive to the magnitude of this parameter. A further increase in the external work inflicts further damage on the material and, eventually, the separation distance reaches its critical value  $\delta_m$ , i.e. the critical crack opening displacement. At this stage the material is fractured and the stresses on the fracture surfaces drop to zero, i.e. they no longer transfer the load across the surfaces. The work done by the cohesive forces is equal to fracture energy,  $G_c$ , of the adhesive material, which was obtained directly from the TDCB tests. The materials' mechanical properties used for the numerical simulations are shown in Tables 3 and 4.

## RESULTS

### *Mechanical Properties*

Families of tensile stress-strain curves have been generated for strain rates in the range of  $10^{-6} - 10 \text{ s}^{-1}$  at  $23^\circ\text{C}$ , for both the epoxy adhesives. These are illustrated in Fig. 4 (a) and (b). The tensile properties were found to increase progressively with the increasing rate. Calculated mechanical properties are summarised in Table 3. The properties of the aluminium alloys are not significantly affected by the rates considered and may be regarded as rate independent [13]. The mechanical properties of the aluminium alloys used in the current research are summarised in Table 4.

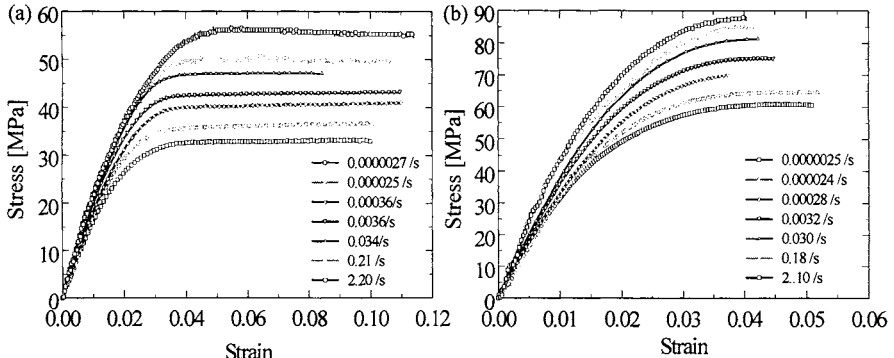


Fig. 4: Tensile stress/strain data for the epoxy adhesives at specified average strain rates, at 23°C: (a) 'XD1493'; (b) 'XD4600'.

Table 3: Tensile properties of the 'XD1493' and the 'XD4600' epoxy adhesives at specified average strain rates, at 23°C. (Typical number of test replicates was four).

Strain rate [s <sup>-1</sup> ]	'XD1493'		'XD4600'	
	UTS [MPa]	Modulus [GPa]	UTS [MPa]	Modulus [GPa]
10 <sup>-6</sup>	33.6 ± 0.6	1.61 ± 0.02	59.8 ± 1.5	3.25 ± 0.07
10 <sup>-5</sup>	36.6 ± 0.9	1.80 ± 0.02	64.1 ± 0.4	3.41 ± 0.09
10 <sup>-4</sup>	40.5 ± 0.5	1.89 ± 0.03	69.6 ± 1.3	3.46 ± 0.17
10 <sup>-3</sup>	42.6 ± 0.9	1.99 ± 0.06	74.1 ± 1.0	3.76 ± 0.13
10 <sup>-2</sup>	47.7 ± 0.6	2.17 ± 0.14	80.9 ± 0.8	4.07 ± 0.47
10 <sup>-1</sup>	49.1 ± 2.3	2.25 ± 0.22	83.2 ± 1.3	4.43 ± 0.37
10 <sup>0</sup>	57.0 ± 1.3	2.38 ± 0.14	88.3 ± 0.6	4.56 ± 0.51

Table 4: Tensile properties of the aluminium alloys employed in the current research obtained at a constant strain rate of 10<sup>-4</sup> s<sup>-1</sup>, at 23°C. (Typical number of test replicates was four).

Alloys	5754-0	6111-T4	2014
Modulus - $E_s$ [GPa]	65.3 ± 0.9	69.8 ± 1.1	71.7 ± 1.0
Yield stress - $\sigma$ [MPa]	98.5 ± 1.0	281.5 ± 0.4	-
Poisson's Ratio - $\nu$	0.33 ± 0.005	0.33 ± 0.008	0.33 ± 0.006

#### Calibration of CZ model parameter $\sigma_m$

As mentioned earlier, the  $G_c$  value required to define the CZ model is obtained from TDCB tests. The remaining parameter  $\sigma_m$  is chosen as the UTS, and was extracted from the stress-strain curves at the corresponding rates. This was an arbitrary choice, since the level of the constraint near the crack tip is higher than that in uniaxial tensile tests used to obtain the stress-strain curves. Therefore, a sensitivity study on this parameter was performed. For illustration purposes, a numerical analysis carried out on TDCB test specimens bonded with the two adhesives under investigation is shown in this section. The value of  $\sigma_m$  was varied from 20 to 80 MPa and numerical predictions of load versus time were compared against the experimental results. Fig. 5 shows a comparison of the FV and experimental results for different  $\sigma_m$  values for TDCB tests performed at 0.1 mm/min. The best fit  $\sigma_m$  value should be able to predict correctly both the experimental force and crack history. (Note that the latter was found to be less sensitive to changes of the cohesive strength.)

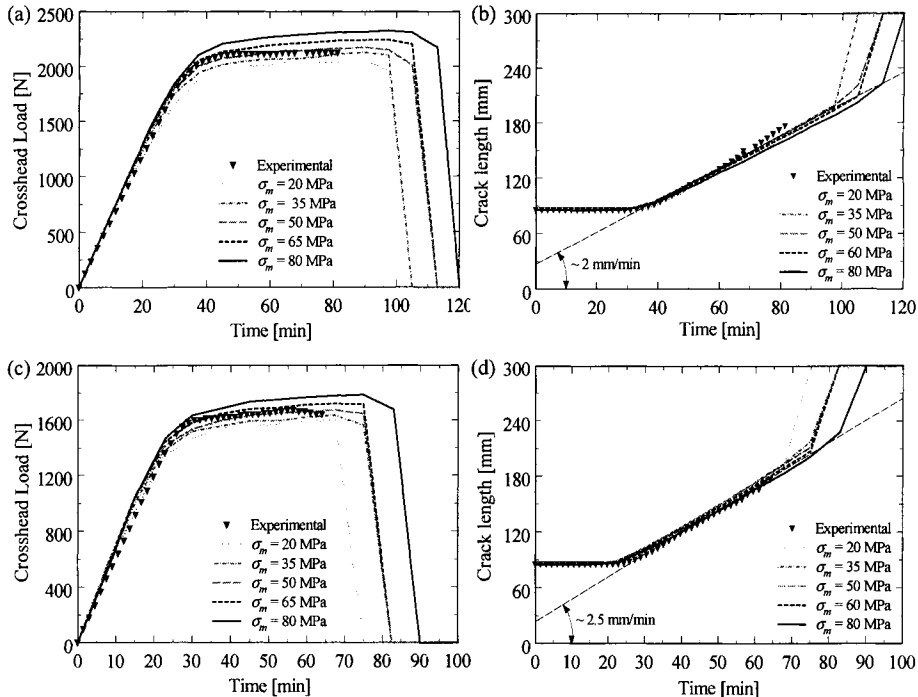


Fig. 5: Comparison of FV and experimental TDCB results obtained at 0.1 mm/min for different  $\sigma_m$  values: (a) Force versus time response of a TDCB specimen bonded with 'XD1493' adhesive,  $G_c = 5037 \text{ J/m}^2$ ; (b) Crack history of a TDCB specimen bonded with 'XD1493' adhesive,  $G_c = 5037 \text{ J/m}^2$ ; (c) Force versus time response of a TDCB specimen bonded with 'XD4600' adhesive,  $G_c = 3043 \text{ J/m}^2$ ; (d) Crack history of a TDCB specimen bonded with 'XD4600' adhesive,  $G_c = 3043 \text{ J/m}^2$ .

It can be seen that for a range of  $\sigma_m$  values close to the UTS values of the two adhesives obtained experimentally at the corresponding strain-rates, i.e.  $10^{-6}$  strains/s, the predicted and experimental results are in very good agreement. The low sensitivity of results to the variation in  $\sigma_m$  assures accurate numerical predictions as long as  $\sigma_m$  is within an acceptable realistic level, i.e. close to the UTS value. A different calibration procedure applicable for quasi-static situations is presented in [14].

#### TDCB Tests

In the low rate tests the crack propagation force, as well as the crack speed, were found to be approximately constant (see Figs. 6(a) and 6(b)), giving a constant value of the adhesive fracture energy with the length of the propagating crack, i.e. no 'R-curve' effects were observed. Initially, the load increased linearly with displacement without affecting the crack length, Fig. 6 (a). Once the critical cohesive stress is reached, a damage zone forms in front of the crack tip (see Fig. 7), resulting in the deviation of the load/displacement curve from a straight line, Fig. 6(a). When the damage zone is increased to the extent where the critical separation distance is reached, the crack starts propagating at a constant speed, Fig. 6(b). Although the profiles of the arms are machined such that the compliance increases linearly with the crack length, the crack propagated in a transient manner soon after the crack front approached the last quarter of the TDCB specimen. Such behaviour was observed in the

experiments and was also predicted by the numerical model. The numerical and experimental results are in very good agreement, both qualitatively and quantitatively, see Figs. 6(a) and 6(b). The choice of  $\sigma_m$  being equal to UTS seems to be satisfactory, as both load-time and crack-length-time data are predicted very well numerically. At higher test rates of 0.5 and 1 m/s, significant changes in the fracture behaviour of the TDCB joints were observed:

- Impact loading conditions cause an early crack initiation or crack tip damage resulting in a decrease of the specimen compliance, as can be seen from the early change in the slope of the force/displacement trace compared to the numerical FV predictions (Fig. 8(a)).
- Dynamic effects occur causing oscillations in the force signal (Fig. 8(a)).
- The type of failure for the 'XD4600' adhesive was found to alter with increasing test rate. Whereas all 'XD1493' adhesive TDCB joints failed in a stable continuous manner, TDCB specimens bonded with the 'XD4600' adhesive showed a transition to stick-slip behaviour at these increased test rates (Fig. 8). It is argued that this is probably due to the strain rate dependent fracture toughness of this adhesive.
- The crack propagation force was also found to increase with increasing test rate. As can be seen from Fig. 8, this was more pronounced in the case of the 'XD1493' adhesive, where a 25% increase in the propagation force value was measured compared to 1 mm/min test presented in Fig. 6(a).

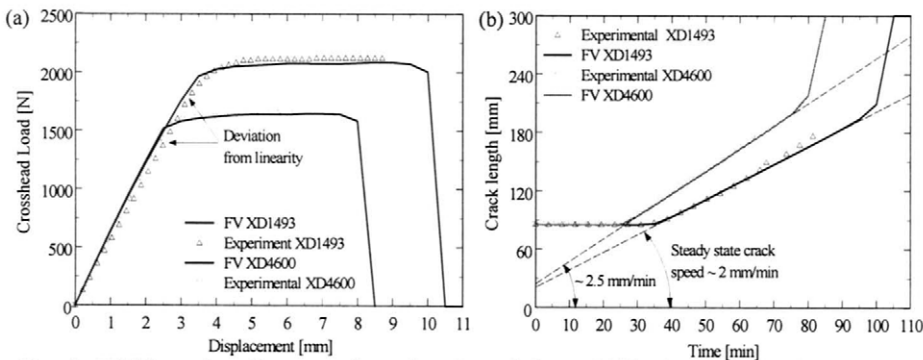


Fig. 6: TDCB results of tests performed at 1 mm/min, at 23°C. Comparison of FV and experimental results: (a) Load/Displacement curves; (b) Crack length histories. CZM parameters: 'XD1493' -  $\sigma_m = 33.6$  MPa,  $G_c = 5037$  J/m<sup>2</sup>; 'XD4600' -  $\sigma_m = 59.8$  MPa,  $G_c = 3043$  J/m<sup>2</sup>.

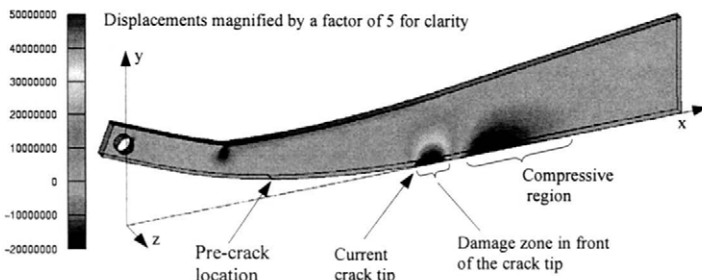


Fig. 7: Normal stress component  $\sigma_{yy}$  [Pa] at time  $T = 75$  min after the beginning of the test in the TDCB FV simulation.

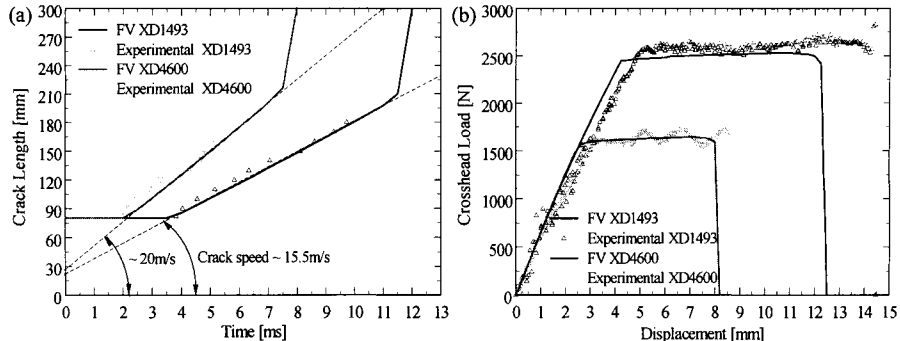


Fig. 8: TDCB results of tests performed at 1 m/s, at 23°C. Comparison of FV and experimental results: (a) Load/Displacement curves; (b) Crack length histories. CZM parameters: 'XD1493' -  $\sigma_m = 54.3$  MPa,  $G_c = 7465$  J/m<sup>2</sup>; 'XD4600' -  $\sigma_m = 86.4$ ,  $G_c = 2981$  J/m<sup>2</sup>.

Numerical results for the high rate TDCB tests are generally in a close agreement with experiments, giving good predictions of the force and crack histories. However, in cases where stick-slip behaviour was observed, e.g. for 'XD4600' adhesive, a rate independent CZ model has not produced satisfactory agreement with experiment, i.e. stick-slip behaviour was not possible to predict for any chosen set of CZ parameters. Results are limited to a quantitative estimation of the average force and crack speed values, (Figs. 8(a) and 8(b)). In order to overcome this problem a crack velocity dependent CZ model was considered. From the analysis of the numerical TDCB results, the crack speed was related to the strain rate values in the process region. Values of  $\sigma_m$  were then extrapolated from available stress-strain data, see Table 3, at the corresponding test rates. Fracture energy values were calculated analytically using the upper and lower bounds of the saw-tooth force versus time trace, assuming that the minimum  $G_c$  value corresponds to the highest crack speed and vice versa. Also, a linear relationship between CZ parameters and the crack speed was assumed, see Fig. 9. A comparison between the numerical prediction, with rate dependent CZ parameters, and the experimental results for a TDCB test performed at 0.5 m/s is illustrated in Fig. 10. Although the agreement is not perfect, the theoretical results clearly predict stick-slip behaviour.

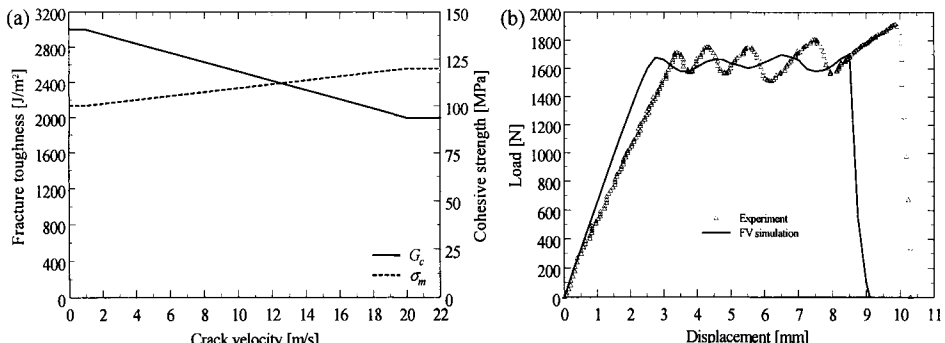


Fig. 9: Velocity dependence of cohesive parameters

Fig. 10: Comparison of FV and experimental results for a TDCB specimen tested at 0.5 m/s

### T-Peel Tests

Typical force versus time traces obtained from T-Peel tests are shown in Fig. 11. As can be seen, the peel load reaches a nearly constant value for both substrate materials, with some minor fluctuations superimposed on the results. These values have been used in an analytical model to calculate the adhesive fracture energy,  $G_c$  [8]. For all the tests performed the crack propagated cohesively in the adhesive layer. The peel load was found to depend on the alloy type and on the thickness of the substrates, since most of the energy during the test is dissipated by plastic deformation of the arms. Numerical FV work is in progress.

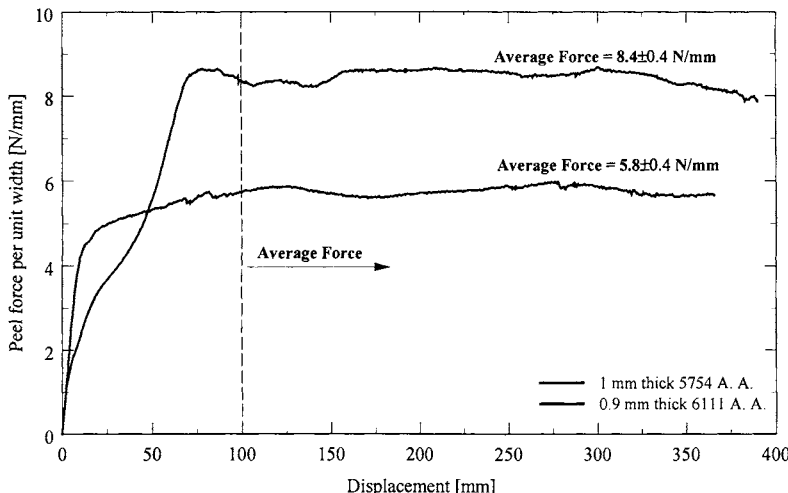


Fig. 11: Force versus displacement response of T-Peel specimens bonded with 'XD4600' adhesive and tested at 5 mm/min, 23 °C.

### IWP Tests

From the tests performed, the crack was always found to propagate cohesively through the adhesive layer of the IWP specimens. The crack propagated either in a transient or in a quasi-static manner, depending on the substrate thickness. Typical IWP force versus time traces for both of these propagation regimes are shown in Fig. 12(a). In the case of quasi-static crack growth (1 mm thick specimens) the presence of two distinct regions, an initial high-peak region followed by a 'plateau' region, can be easily detected. From a careful examination of the high-speed photography results, it can be speculated that the main causes for these initial peaks are dynamic effects, which arise from (a) the initial contact between the wedge and the specimen, and (b) crack initiation from the bead of adhesive that was formed in the 'V' of the specimen.

This was further examined with a series of tests performed on specimens with a pre-crack. Specimens with a PTFE tape of 10 mm length inserted in the adhesive, experienced significant reduction of the initial peak (see Fig. 12(b)). In the case of the quasi-static crack growth, the crack speed, within the 'plateau' region, was found to be equal to the test rate. In the case of the transient crack growth (2 mm thick specimens), again the initial region of the force versus time response consists of one or more peaks, due to the same reasons as before. However, this time rapid crack propagation takes place, and the absence of the 'plateau' region can be clearly seen in Fig. 12(a).

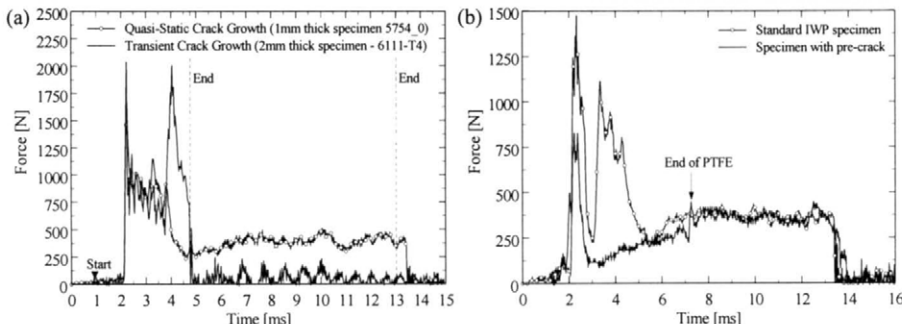


Fig. 12: Force versus time response from IWP specimens showing stable and unstable crack growth (a) Standard IWP specimen; (b) IWP specimen with a pre-crack.

The reason for this behaviour is that in the case of the thicker and, therefore, stiffer substrate materials, a larger amount of energy was elastically stored in the substrates prior to crack initiation. Hence, after the onset of the crack growth, the rate of energy release would be much higher than that required for quasi-static crack growth, resulting in the transient crack propagation. Here, the crack velocities were much higher than the test rate. Analysis of the high-speed photographs has shown a crack velocity of 26 m/s for a test conducted at 2 m/s (see Fig. 13). Careful examination of the failed specimens revealed that the main characteristics of quasi-static crack growth were the large plastic deformation of the substrate arms and the associated high-energy dissipation. In contrast, specimens that exhibited transient crack growth showed no plastic deformation and, as would be expected, very low energy dissipation.

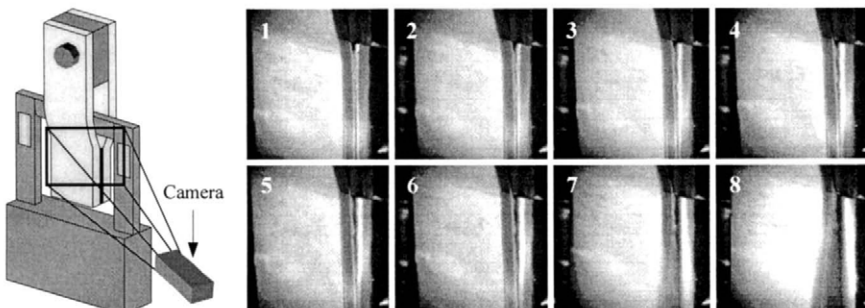


Fig. 13: High-speed photography of an IWP test which exhibited transient crack growth. Aluminium 6111-T4 series bonded with 'XD4600' adhesive and tested at 2 m/s, 23°C. The inter-frame time was 222 µs.

A preliminary numerical simulation of the IWP tests was performed assuming linear-elastic behaviour for both the adhesive and the substrates. Two different geometries (i.e. 1 and 2 mm thick substrates) were modelled at an impact speed of 2 m/s. The model used the traction-separation obtained from the TDCB numerical results. Although the analysis was limited to elastic materials, the numerical observations were qualitatively in a good agreement with the experiments. The numerical simulations predicted that in the case of thin specimens the crack was driven by the wedge at the test rate, whereas in the case of thick substrates the crack was predicted to propagate in a transient manner. The calculated crack speed was also in qualitative agreement with that measured from the high-speed photography.

## CONCLUSIONS

Experimental results obtained from various tests have demonstrated the effects of loading rates on both the basic mechanical and fracture properties of adhesive joints. The 'XD1493' adhesive joints showed an increase in the fracture toughness from about  $5 \text{ kJ/m}^2$  at 1 mm/min loading rate, to about  $7.5 \text{ kJ/m}^2$  at 1 m/s. On the other hand, the average value of  $G_c$  did not change considerably with test rate for the 'XD4600' adhesive joints, but stick-slip behaviour was observed at rates above 0.5 m/s. A general method of calibrating CZ parameters was established. It is based on  $G_c$  values calculated from the TDCB results, while the value of  $\sigma_m$  was chosen being equivalent to the UTS from the stress-strain curves at the appropriate rate. The 'fine-tuning' of this parameter was achieved by numerically fitting the measured load-displacement curves and the crack length histories. A novel rate dependent CZ model was developed and successfully applied for predicting the stick-slip behaviour of the 'XD4600' TDCB joints. Numerical predictions of the IWP tests, where the CZ parameters from TDCB tests were employed, were very encouraging. Further work on modelling the IWP and T-peel tests, including large strain plasticity, is in progress. The work will help to clarify the issue of transferability of the CZ parameters between the TDCB and the peel geometries, which is still an issue of some debate.

## ACKNOWLEDGEMENTS

The authors wish to acknowledge funding and support from the following companies and organizations: ALCAN Int., DERA, EPSRC and FORD Motor Company. They would also like to thank Mr. Aleksandar Karac for his contribution in the development of the numerical procedure for predicting stick-slip behaviour.

## REFERENCES

1. W. S. Miller, L. Zhuang, J. Bottema, A. J. Wittebrood, P. De Smet, A. Haszler and A. Vieregge, *J. Mater. Sci. and Eng.* **A280** (2000) 37
2. B.R. K. Blackman, A. J. Kinloch, A. C. Taylor and Y. Wang, *J. Mater. Sci.* **35** (2000) 1867
3. American Society for Testing and Materials, *ASTM E 8M - 89b* (1986)
4. American Society for Testing and Materials, *ASTM D 638 - 72* (1972)
5. European Standard EN ISO 2818. Plastics, CEN European Committee for Standardisation (1999)
6. International Standards Organisation, *ISO 15166-1* (1998)
7. S. Mostovoy, P. B. Crosley and E. J. Ripling, *J. Materials* **2** (1967) 661
8. I. Georgiou, H. Hadavinia, A. Ivankovic, A. J. Kinloch, V. Tropsa and J. G. Williams, *J. Adhesion*, in press
9. International Standards Organisation, *ISO 11343* (ISO, Geneva, 1993)
10. EPSRC. Web page Address: [www.eip.rl.ac.uk](http://www.eip.rl.ac.uk)
11. A. Ivankovic, *Computer Modelling and Simulation in Engineering* **4** (1999) 227
12. H. G. Weller, G. Tabor, H. Jasak and C. Fureby, *Computers in Physics* **12** (1999) 620
13. The Aluminium Association, Publication, AT6 (1998)
14. T. Ferracin, C. Landis, F. Delannay and T. Pardo, Proc. 10<sup>th</sup> International Conf. on Fracture – ICF10, Hawaii, USA, Dec. 2001.